Preprint typeset in JHEP style - HYPER VERSION

arXiv:1703.05139v1 [astro-ph.CO] 15 Mar 2017

Strongly Coupled Dark Energy with Warm dark matter vs. LCDM.

Silvio A. Bonometto, Marino Mezzetti

INAF, Osservatorio di Trieste & Trieste University, Physics Department, Astronomy Unit, Via Tiepolo 11, 34143 Trieste, Italy

Roberto Mainini

Physics Department G. Occhialini, Milano–Bicocca University Piazza della Scienza 3, 20126 Milano, Italy

Abstract: Cosmologies including strongly Coupled (SC) Dark Energy (DE) and Warm dark matter (SCDEW) are based on a conformally invariant (CI) attractor solution modifying the early radiative expansion. Then, aside of radiation, a kinetic field Φ and a DM component account for a stationary fraction, $\sim 1\,\%$, of the total energy. SCDEW models alleviate conceptual problem of LCDM, while recovering its results, and even easing some LCDM problems, below the average galaxy scale. The CI expansion begins at the inflation end, when Φ (future DE) possibly plays a role in reheating, and ends at the Higgs' scale. Afterwards, a number of viable options is open, allowing for the transition from the CI expansion to the present Universe. In this paper: (i) We show how the attractor is recovered when the spin degrees of freedom decreases. (ii) We perform a detailed comparison of CMB anisotropy and polarization spectra for SCDEW and LCDM, including tensor components, finding negligible discrepancies. (iii) Linear spectra exhibit a greater parameter dependence at large k's, but are still consistent with data for suitable parameter choices. (iv) We also compare previous simulation results with fresh data on galaxy concentration. Finally, (v) we outline numerical difficulties at high k. This motivates a second related paper, where such problems are treated in a quantitative way.

Contents

1. Introduction **1**

2. Coupled DE in the early Universe. Background components **3**
- 2.1 A kinetic tracker solution 3
- 2.2 Coupled cosmologies with fixed $w(a)$ 4
- 2.3 Lagrangian interactions and inflationary reheating 5
- 2.4 DM field components, Higgs mass acquisition, and coupling late fading 6

3. A common origin for DM components? **9**

4. Linear fluctuation evolution **11**
- 4.1 CMB 12
- 4.2 Linear spectra 13
- 4.3 Linear and non–linear fluctuation evolution 16

5. Discussion **19**

1. Introduction

LCDM models account for a large deal of data, well beyond cosmic acceleration and background component distribution. In turn, they have fine tuning and coincidence problems. Accordingly, it is reasonable to take them as a sort of highly performing *effective* models.

It is possible that the true physics laying behind LCDM has to do with limits to General Relativity (GR) validity [1], namely at large scales or low densities. Reality could be even more awkward, involving further dimensions or colliding branes [2].

Here we discuss a less intriguing option, with a feature in common with several previous suggestions [3, 4], i.e. that Dark Energy (DE) is a scalar field Φ, so exploiting a specific feature of these fields when self–interacting: a negative pressure approaching their energy density ($|p_\Phi| \sim |\rho_\Phi|$).

Apart of that, our option, dubbed SCDEW (Strongly Coupled Dark Energy plus Warm dark matter), exhibits key differences from former models: (i) Starting from the finding of an early conformally invariant (CI) attractor, SCDEW includes a stationary contribution $\mathcal{O}(1\,\%)$ of Φ and Dark Matter (DM), *all through radiative eras*; in fact, if uninteracting, cold DM and a kinetic scalar field Φ would dilute as a^{-3} and a^{-6}, respectively; SCDEW allows for a suitable energy flow from DM to Φ, so that both components dilute as a^{-4}, in parallel with radiation, along the attractor. (ii) Φ, besides of yielding DE, has a role in post–inflationary reheating; this is a new point illustrated in this work; the option of Φ

being itself the inflaton is not discussed here. (iii) Today, Φ must be self–interacting, but the shape of the self–interaction potential $V(\Phi)$ is unessential and its (hard) determination is not a test for SCDEW models. (iv) SCDEW includes two Dark Matter (DM) components, that we dubb coupled and warm (cDM and WDM, respectively). The coupling with Φ of cDM is *initially* quite strong, as will be detailed shortly.

Moreover, WDM and cDM naturally share close primeval densities and, in this paper, we shall debate only cases when they have an equal mass $\mathcal{O}(100\,\mathrm{eV})$.

Some previous papers [6, 7, 9] were already devoted to SCDEW cosmologies; n–body simulations based on them were also performed [10], finding substantial improvements in the description of scales below the average galactic scale, in respect to LCDM (a new comparison with recent galactic concentration data is also included in this paper). Apart of resuming the basic features of SCDEW models, this paper is focused on two points: the possible role of Φ in post–inflationary reheating and a model upgrade allowing a low–z fading of coupling.

A number of side results will be also presented. In particular, we provide detailed information on how model parameters influence matter fluctuation spectra $P(k, z)$ at low redshift z. Such parameters are essentially 2, accounting for Φ–DM coupling and WDM particle mass. Recent data (e.g., high–z Lyman–α clouds [11], or the Hubble telescope and Planck H_0 values [12]) put constraints on them, in a way we shall indicate. A stringent quantitative analysis is however postponed to further work.

The possibility of a common origin for DM components is also debated here. This is related to the CI attractor behavior when the fall of cosmic temperature yields a decrease in the number of effective spin degrees of freedom

$$g = \frac{7}{8}\mathcal{N}_{fermion} + \mathcal{N}_{boson}\ . \tag{1.1}$$

Here $\mathcal{N}_{fermion,boson}$ is the number of fermion, boson relativistic spin states. The problem will be illustrated here by showing the attractor behavior at the Quark–Hadron transition, occurring at a temperature $T_c \sim 170\,\mathrm{MeV}$, when g decreases by ~ 61.75 to ~ 14.25 (with 3 neutrino species) as, then, the contribute of strongly interacting particles falls to almost nil (pion density is strongly suppressed by their physical size, while baryon masses are $\gg T_c$).

Another point of this work is a detailed comparation of SCDEW and LCDM anisotropies and polarization for CMB, also in presence of a tensor signal.

We shall finally motivate a second related paper [8], where the behavior of early non–linearities in cDM will be debated, finding that, far from yielding early bound systems, a fear outlined in [9], they are expected to cause fluctuation dissipation, so yielding a low–scale spectral cutoff, around 10–100 $M_\odot$. It may be worth comparing this cutoff scale with the expected spectral cutoff in ordinary LWDM models, if including DM particles of mass $\sim 100\,\mathrm{eV}$: in such case the $P(k, z)$ cutoff lays well above large galaxy mass scales.

The plan of the paper is as follows: In the next Section we shall first resume the SCDEW cosmology scheme, then outlining the mechanism allowing to exit the CI expansion regime though the Higgs' mass acquisition by the coupled spinor field. This is the basic new idea we develop in this work and the vicinity, between the Higg's mass advisable

for the warm DM component and such mass, suggested us to debate, in Section 3, the possibility that the 2 fields are somehow directly related. In the same Section we also show how the kinetic attractor is recovered when the effective number of relativistic spin degrees of freedom varies. Section 4 is then devoted to discuss the linear fluctuation evolution in this version of SCDEW cosmologies. We therefore show in detail the (snall) discrepancies between LCDM and SCDEW in CMB spectra, as well as the more significant discrecancies in the linear fluctuation spectra, however showing that this model cathegory requires a treatment more complicated than a linear program extension, to treat the high–k expectations. We conclude the paper with a discussion section.

2. Coupled DE in the early Universe. Background components

2.1 A kinetic tracker solution

The state equation of a purely kinetic scalar field Φ, whose *free* Lagrangian

$$\mathcal{L}_f \sim \partial^\mu \Phi \partial_\mu \Phi \ , \tag{2.1}$$

is $w = p_k/\rho_k \equiv 1$ ($p_k,\ \rho_k$: field kinetic pressure, energy density). Accordingly, $\rho_k = \dot{\Phi}^2/2a^2$ dilutes $\propto a^{-6}$. Here a is the scale factor appearing in the background metric

$$ds^2 = a^2(\tau)(d\tau^2 - d\lambda^2) \ , \tag{2.2}$$

τ being the *conformal time* and λ being the *comoving distance*. Dots indicate differrentiation with respect to τ, all through the paper.

It is also known that non–relativistic DM density $\rho_c \propto a^{-3}$, its state parameter being $w = 0$. Accordingly, it appears rather intuitive that a suitable energy flow from DM to Φ could speed up DM dilution while ρ_k dilution slows down, so that both dilute $\propto a^{-4}$. If the overall expansion is radiation dominated (RD), this yields constant early density parameters Ω_c and Ω_d (for DM and Φ, respectively). The shift required, for the dilution exponent of the kinetic energy of the field Φ, is double in respect to DM exponent shift. Therefore, also intuitively, we expect such effect to require that $\Omega_c = 2\,\Omega_d$.

As a matter of fact, in [6] it was shown that these expectations are consistent with a DM–Φ coupling ruled by the equations

$$T^{(d)\ \mu}_{\ \ \nu;\mu} = +CT^{(c)}\Phi_{,\nu} \ , \qquad T^{(c)\ \mu}_{\ \ \nu;\mu} = -CT^{(c)}\Phi_{,\nu} \ , \tag{2.3}$$

an option introduced since the early papers on DE [4], aimed there to ease DE fine tuning and coincidence problems *in the present epoch,* i.e. after radiation dominated expansion end. This option gave origin to a vaste literature and simulations of these models were also compared with data [5]. These equations will be however used here in a fully different context.

Let us then outline that, in eq. (2.3) $T^{(c,d)}_{\mu\nu}$ are the stress–energy tensors of the DM and Φ field components, $T^{(c)}$ is the trace of the former tensor while

$$C = b/m_p = (16\pi/3)^{1/2}\beta/m_p \tag{2.4}$$

(m_p : the Planck mass) is the DM–DE coupling constant.

As a matter of fact, these very equations, used now in the early *radiative expansion*, allowed [6] to show that, if the early density parameters are

$$\Omega_c = 2\,\Omega_d = \frac{1}{2\beta^2}\ , \tag{2.5}$$

we are on an attractor: if we start from DM and Φ components which exhibit initial densities not fultilling eq. (2.5), their densities rapidly modify finally settling on such *conformally invariant* solution which is, therefore, a *kinetic tracker solution* in the radiation dominated epoch.

In Section 3 we shall again check the attractor efficiency, by reporting the evolution of coupled DM and DE while the cosmological Quark–Hadron transition led to a sudden decrease of the spin degrees of freedom in the radiative component. Here we shall partially review results obtained in a previous paper [15], by treating, however, different parameter ranges.

In the frame of reference where the metric is (2.2), eqs. (2.3) read

$$\ddot{\Phi} + 2\frac{\dot{a}}{a}\dot{\Phi} = -a^2 V'_\Phi + Ca^2\rho_c\ , \qquad \dot{\rho}_c + 3\frac{\dot{a}}{a}\rho_c = -C\rho_c\dot{\Phi}\ , \tag{2.6}$$

$V(\Phi)$ being a self–interaction potential density for the Φ field which, however, is nil or negligible along the kinetic tracker solution.

These equations, with selected $V(\Phi)$ potentials, allow for high–z tracker solutions. They belong to the approach cited hereabove [4, 5]. The attractor considered herebelow is for a purely kinetic Φ field, so that the potential shape is fully irrelevant.

2.2 Coupled cosmologies with fixed $w(a)$

The quest for an expression of the $V(\Phi)$ potential, in this context, might comes much after. Present and future observations [16, 17, 18], however, more directly constrain the state parameter $w(a)$, rather than $V(\Phi)$. Accordingly, in [6], it was shown that the eqs. (2.6) also read

$$\dot{\Phi}_1 + \tilde{w}\frac{\dot{a}}{a}\Phi_1 = \frac{1+w}{2}Ca^2\rho_c\ , \qquad \dot{\rho}_c + 3\frac{\dot{a}}{a}\rho_c = -C\rho_c\Phi_1\ , \tag{2.7}$$

while

$$2\tilde{w} = 1 + 3w - \frac{d\ln(1+w)}{d\ln a} \tag{2.8}$$

and $\Phi_1 \equiv \dot{\Phi}$. These equations aim to tell us Φ evolution directly from $w(a)$ dependence. Notice that they do not involve the undifferentiated field Φ, so that the whole system is just second order, and $w(a)$ information always admits an arbitrary additional constant on Φ.

This approach simplifies our analysis also for the very–early Universe context, when we assume $w \equiv 1$ (purely kinetic field) and a radiative expansion. At a suitable low redshift, however, there must be a transition from kinetic to potential dominance, so that the Φ can account for a component with $w \simeq -1$ today.

This is not an *ad–hoc* feature of SCDEW. Also coupled DE approaches based on specific potentials (e.g., a SUGRA or RP) require a fast transition of Φ from potential to kinetic

regime above a suitable z_{kp}, unless a very low β ($\lesssim 10^{-3}$) is selected. Examples were shown in previous work, so that requiring

$$w(a) = \frac{1-A}{1+A} \quad \text{with} \quad A = \left(\frac{a}{a_{kp}}\right)^{\epsilon} \ , \tag{2.9}$$

as suggested in [7], will hardly contradict any data in the next decades; here $a_{kp} = 1/(1 + z_{kp})$. Selecting ϵ is then as choosing a potential expression. The very dependence on ϵ of results is however extremely mild (see again [7]) and all through this paper we take $\epsilon = 2.9$.

2.3 Lagrangian interactions and inflationary reheating

Once we assume $w \equiv 1$ during the radiative expansion, eqs. (2.7) can be soon integrated, yielding the above mentioned kinetic tracker solution

$$\Phi_1 = 1/C\tau \ , \qquad \rho_c = \bar{\rho}_c(\bar{a}/a)^4 \ , \tag{2.10}$$

wherefrom we deduce that

$$C\Phi = \ln(\tau/\bar{\tau}) \tag{2.11}$$

Φ being again undetermined for an arbitrary additive constant; in other terms, we ignore the field value at $\bar{\tau}$; $\bar{\rho}_c$ and $\bar{a}$ are the energy density and the scale factor at $\bar{\tau}$.

In [9] it was then shown that the coupling term in eqs. (2.6) or (2.7) derives from a generalized Yukawa interaction Lagrangian

$$\mathcal{L}_m = -\mu f(\Phi/m)\bar{\psi}\psi \tag{2.12}$$

provided that

$$f = \exp(-\Phi/m) \ . \tag{2.13}$$

Here 2 indipendent mass scales, $m = m_p/b$ and $\mu = g\, m_p$ need to be introduced for dimensional reasons. The constant b coincides with the factor b gauging the DM–Φ interaction strength in eq. (2.4), so that $C = b/m$; on the contrary, g keeps undetermined as well as a Φ additive constant. Here, the spinor field ψ accounts for interacting DM, its particle number density operator being $n \propto \bar{\psi}\psi$. From this lagrangian density we work out the energy density

$$\rho_c = \mu f(C\Phi)\bar{\psi}\psi \ , \tag{2.14}$$

(formally $= -\mathcal{L}_m$) for DM spinor quanta, which are non–relativistic. It is then worth focusing on the term

$$\frac{\delta\mathcal{L}_m}{\delta\Phi} \equiv [\mathcal{L}_m]'_\Phi = -\mu f'_\Phi(C\Phi)\bar{\psi}\psi = -\frac{f'_\Phi(C\Phi)}{f(C\Phi)}\rho_c = C\rho_c \tag{2.15}$$

of the Euler–Lagrange equation which, multiplied by a^2, is the second term at the r.h.s. of the first eq. (2.6) (let us remind that $C = b/m_p$). This will become a critical point when we shall consider the effects of Higgs mass acquisition by the different fields.

Meanwhile, let us notice that

$$\rho_c \propto f(C\Phi)a^{-3}, \tag{2.16}$$

according also to the findings in [13], as indeed $n \propto a^{-3}$. Taking into account the expression (2.11) of Φ, we then confirm that

$$\rho_c a^4 = \bar{\rho}_c \bar{a}^4 \tag{2.17}$$

during the radiative era.

Let us now consider the coupling (2.12) within the context of large–field inflation. We can imagine that, around Planck time, the "initial" $\Phi = F \times m_p$ with $F = 3$–4 . From the expressions (2.12) and (2.13), we see that the interaction lagrangian, initially reading

$$\mathcal{L}_m \simeq -\mu \exp(-Fb)\bar{\psi}\psi \tag{2.18}$$

is then strongly suppressed (namely if b values are large, yielding a later very strong coupling) and the interaction acquires strength only when Φ rolls down to values $\sim m_p$ or less. Let us state that elsehow: The Lagrangian (2.18) yields two equilibrium configurations: $\Phi \to \infty$ and Φ on the CI solution. During inflation, the former equilibrium is approached; but Φ decrease drives away from it, finally favoring reheating; Φ decrease, however, does not proceed to nil: it stops when the latter configuration is attained.

Accordingly, the lagrangian (2.18) should not account for the slow rolling down process itself, just in the same way as, later on, it shall not account for DE energy density. On the contrary, it accounts for fastly turning the Φ field energy into DM, i.e. into ψ quanta, as it occurs during the reheating; then, later on, it accounts for the same process at a suitably tuned slow rate, in the stationary expansion regime. Until such regime is reached, this very process will receive further quantum contributions from the symultaneous evolution of the vacuum state, accounted for by Bogoliubov transformations, a process also stopping at the reach of the stationary expansion regime along the attractor, in a conformally invariant (CI) evolution.

The potential term driving the inflationary process could rather (at least partially) coincide with the one yielding DE. This however requires a suitable evolution of the constant(s) it contains, so that the passage of Φ from potential to kinetic dominance (and viceversa) occurs at different Φ values. Owing to the logarithmic evolution of Φ (2.11), however, the constant(s) are just required to evolve logarithmically, as can be consistent with renormalization group expectations.

A toy model possibly accounting for these behaviors is being analysed and will be discussed in a forthcoming paper.

2.4 DM field components, Higgs mass acquisition, and coupling late fading

The relation between the Lagrangian (2.12) and the post–inflationary reheating was not outlined in previous work. Rather, we treated such Lagrangian as just yielding a peculiar z–dependent mass term for the DM field ψ.

Another DM component, made of low mass $\mathcal{O}(100\,\mathrm{eV})$ quanta (of a second spinor field ψ_1), was then introduced. It was then noticed that, if ψ_1 quanta have a mass in such range, the two DM components unavoidably share close primeval densities.

As is natural to expect that ψ_1 quanta acquired such mass m_w at the electroweak (EW) transition scale, through the Higgs mechanism, here we shall suppose that also ψ

acquires a similar mass at the same scale. There is no specific reason to suppose that ψ and ψ_1 will share identical mass values, an assumption somehow envisaging a related nature of the two dark components, but we can exploit the model degrees of freedom and keep to such an option, to select model parameters for this work.

The point is that ψ acquiring a Higgs mass bears critical consequences for the later evolution of DM–DE coupling and, through it, for today's component densities. In fact, at $T < T_{EW}$, the lagrangian (2.12) becomes

$$\tilde{\mathcal{L}}_m = -[\mu f(\Phi/m) + \tilde{\mu}]\bar{\psi}\psi \equiv -\mu[\exp(-C\Phi) + \tilde{\mu}/\mu]\bar{\psi}\psi \ . \tag{2.19}$$

By using this lagrangian we can then re–do the functional differentiation operation in eq. (2.15), so obtaining

$$\frac{\delta\tilde{\mathcal{L}}_m}{\delta\Phi} = -\frac{f'(C\Phi)}{f(C\Phi) + \tilde{\mu}/\mu}\rho_c = \frac{C}{1 + \mathcal{R}\exp[C(\Phi - \bar{\Phi})]}\rho_c \ . \tag{2.20}$$

Here

$$\mathcal{R} = (\tilde{\mu}/\mu)\exp(C\bar{\Phi}) \ , \tag{2.21}$$

$\bar{\Phi}$ being the value of the field at a suitable reference time, e.g. during the stationary regime. However, rather than setting a value for $\bar{\Phi}$, it is more convenient to introduce a coefficient g_h such that

$$\exp(C\bar{\Phi}) = \mu/(g_h m_p) \tag{2.22}$$

so yielding

$$\mathcal{R} = \tilde{\mu}/(g_h m_p) \ . \tag{2.23}$$

Let us also outline that, if the reference time is changed from $\bar{\tau}_1$ to $\bar{\tau}_2$, both assumed to belong to the C.I. expansion epoch, it shall be

$$\mathcal{R}_1 = \mathcal{R}_2\bar{\tau}_1/\bar{\tau}_2 \quad \text{and} \quad g_{h,1} = g_{h,2}\bar{\tau}_2/\bar{\tau}_1 \ . \tag{2.24}$$

The key point, however, is that the dynamical equations, even in the presence of a Higgs' mass for the ψ field, keep the forms (2.6) or (2.7), provided that we perform the replacements

$$C \to C_{eff} = \frac{C}{1 + \mathcal{R}\exp[C(\Phi - \bar{\Phi})]} \quad \text{and/or} \quad \beta \to \beta_{eff} = \frac{\beta}{1 + \mathcal{R}\exp[C(\Phi - \bar{\Phi})]} \ . \tag{2.25}$$

Then, as soon as the Φ increase causes $\Phi - \bar{\Phi}$ to approach $-\ln(\mathcal{R})/C$, the denominators in eq. (2.25) differ from unity, so suppressing the effective coupling intensity. This gives a new dynamical significance to the value of Φ : in the absence of the Higgs mass $\tilde{\mu}$, it would be significant only after kinetic–potential transition, at the eve of the present epoch, and, possibly, before the potential–kinetic transition, in the late inflationary expansion.

Numerical results are then obtainable by integrating the system made by eqs. (2.7), the Friedmann equation, and the "trivial" equation $d(\Phi - \bar{\Phi})/d\tau = \Phi_1$, once the β shift (2.25) is done.

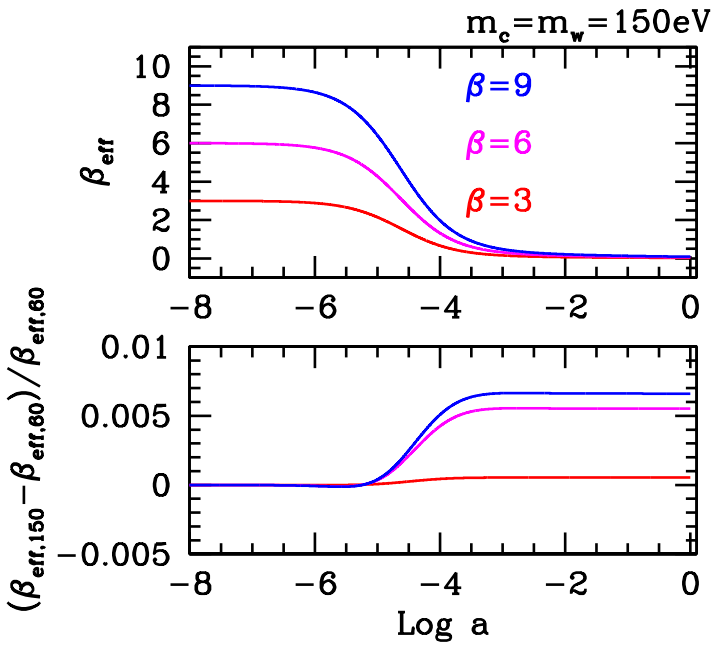


Figure 1: Scale dependence of the effective coupling in SCDEW cosmologies with $m_w = 100\,\mathrm{eV}$ for various couplings β.

In order to set initial conditions, we may then ideally extend the C.I. regime down to the Planck time τ_p, so setting the initial field value $\Phi_i = \Phi_p \ln(\tau_i/\tau_p)$, while we take $g_h = 2\pi$. In order to have $\tilde{\mu} = \mathcal{O}(100\,\mathrm{eV})$, we then have $\mathcal{R} \sim 10^{-27}$, a typical value for the ratio between heavy neutrino and Planck mass scales.

The decline of β_{eff} is illustrated in Figure 1. In Figure 2 we then show the values β_0

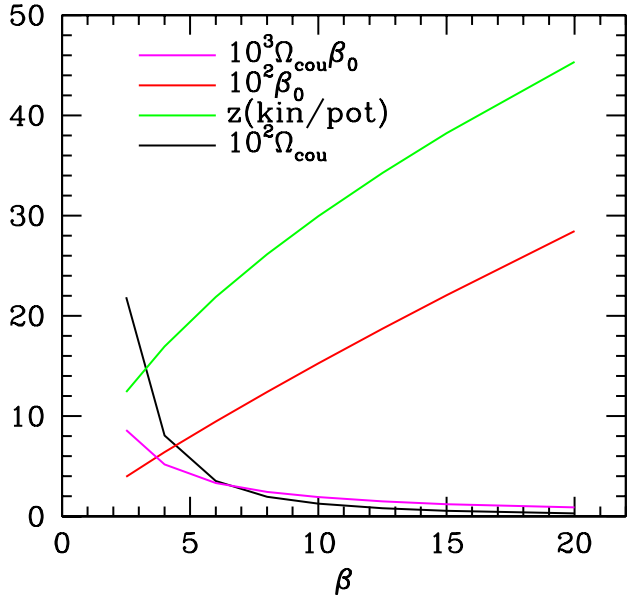


Figure 2: For various (high–z) couplings β and $m_w = 100\,\mathrm{eV}$, we plot the $z = 0$ values of β_0 and Ω_{cou}. The redshift where the kin–pot transition must occur are also plotted.

attained by coupling at $z = 0$ for $\tilde{\mu} = 100\,\mathrm{eV}$. For such $\tilde{\mu}$, even for $\beta = 20$ the coupling at $z = 0$ does not overcome 0.3 (notice that low–z limits on coupling [12] do not apply to this case, as cDM is not the only DM component). The Figure also shows the density parameter $\Omega_{0,cou}$ of coupled DM at $z = 0$, so outlining that, starting from a significant fraction of the total cosmic DM when $\beta \sim 3$, it accounts for < 2–$3\,\%$ of DM (itself accounting for $\sim 25\,\%$ of cosmic density) for $\beta >\sim 8$. If we consider the product $\beta_0\Omega_{0,cou}$, we see that it is also gradually decreasing. This product gauges the "average coupling" of the whole (warm and cold) DM, whose total density parameter is kept constant in the models considered.

It is also worth outlining that results shown in this work are obtained by assuming $\Omega_d = 0.7$, $\Omega_b = 0.045$, Hubble constant $h = 0.685$, $T_0 = 2.726\,\mathrm{K}$, optical depth 0.089, $n_s = 0.986$ and 3 (almost massless) neutrino species.

3. A common origin for DM components?

Taking "equal" Higgs masses for the two DM components (coupled and uncoupled) alludes to their possible common nature, as though they would differ just in the strength of the coupling to Φ. In turn, this option follows from the observation that viable SCDEW models are mostly characterized by close densities of the 2 DM components at high z.

This last effect, however, requires a deeper analysis. Let us suppose, e.g., that the component uncoupled to Φ decoupled from all other cosmic components at a suitable redshift z_d. At that time it is reasonable to expect $\rho_w \simeq \rho_c$ (ρ_w, ρ_c : uncoupled and coupled DM densities, respectively). Later on,

$$\rho_w(z) = \rho_w(z_d)\ \ [(1+z)/(1+z_d)]^4 \tag{3.1}$$

until derelativization. On the contrary, $\rho_c(z) \simeq \rho_{cr}(z)/2\beta^2$ ($\rho_{cr}(z)$: critical density at z). As a consequence of entropy conservation, at any decrease of g (defined in eq. 1.1) after z_d, ρ_{cr} has therefore a jump upward $\propto g^{-1/3}$ and, although after a suitable time delay, ρ_c is bound to accompany such shift, to keep on the attractor.

A major decrease of g unavoidably occurs at the quark–hadron (QH) transition, at a redshift z_c, when the cosmic temperature $T_c \sim 170\,\mathrm{MeV}$ [14], as strongly interacting components cease to be a part of the thermal soup (only pions have a mass $< T_c$, although slightly so; hadron components however have a proper volume, and statistical expressions for pointlike particles can be applied to them only when *co*volume does not matter). For a detailed analysis of the density jump, however yielding a g shift from 61.75 down to ~ 14.25, see [15]. In Figure 3 we show the oscillations of the ratio $(\rho_c + \rho_d)/\rho_r$, before the recovery of the attractor pattern, with radiation density still including neutrinos and electrons; in the plot electron–positron annihilation into photons is omitted, so to outline the only effect of QH transition. A minor quantitative error, made in [15], is also corrected. The detailed shape of the $(\rho_c+\rho_d)/\rho_r$ oscillations slightly depend on specific assumption on the transition and in some case they can propagate down to primeval nucleosynthesis (BBN) [15]. All lattice QCD results currently converge to state that it was a crossover transition. To obtain the results plotted, however, we assumed a transition slightly delayed, until the reactions allowing 3 quarks to coalesce within single baryons could perform their duty. For

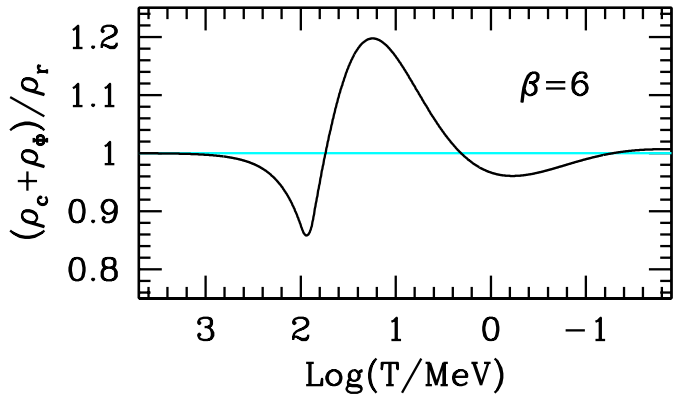


Figure 3: Time evolution of the ratio between densities of coupled DM plus Φ and radiation, in the proximity of the QH transition, for a SCDEW cosmology (with $m_w = 100$ and $\beta = 6$), normalized to $3/4\beta^2 = 0.02083$. The attractor is recovered after a few oscillations, which could however affect BBN redshift range. For $\beta = 6$, effects on BBN are approximately one quarter of what is due to electron–positron annihilation.

other assumptions concerning the transition, see again [15]. Incidentally, let us recall that coupled components, yielding a fractional contribution to cosmic density $\sim 3/4\beta^2$, would have an impact on BBN similar to half neutrino species for $\beta \simeq 3.2$; for the greater β values we consider, therefore, there is no appreciable direct impact. On the contrary, the residual deviations from a purely radiative $a(\tau)$ law, as shown at the r.h.s. of Figure 3, are approximately half of those due to electron–positron annihilation; the impact of such extra deviation is probably negligible but was never directly tested.

Although delayed, the ρ_c growth however means that a common origin of DM components requires that, at the eve of derelativization, it must be $\rho_w < \rho_c$. If $z_d > z_c$, as expected, taking into account also muon later annihilation, we have an upward jump for ρ_c by a factor $\simeq 1.63$. Taking also into account other earlier particle annihilations successive to z_d, common origin requires ρ_w values to lay significantly below ρ_c, in the late CI expansion.

In Figures 4 the evolution of densities in four models compatible with such conditions are shown. These Figures extend to high z without taking into account g variations, as those outlined in the previous Figure. Let us then also outline the progressive increase of β with $m_{c,w}$, in the models shown, assuring that the ratio ~ 1.63 (between high–z coupled DM and warm DM densities) is not badly bypassed (we however neglected the possibility that the number of spin states of the two components are different). SCDEW models badly violating the "1.63" limit, however, need a different explanation for the apparent vicinity of high–z values of ρ_w and ρ_c. The point, however, is that low–β and high mass values seem disfavored by data fits; the idea of a common nature of the DM components, although fascinating, seem therefore uneasy.

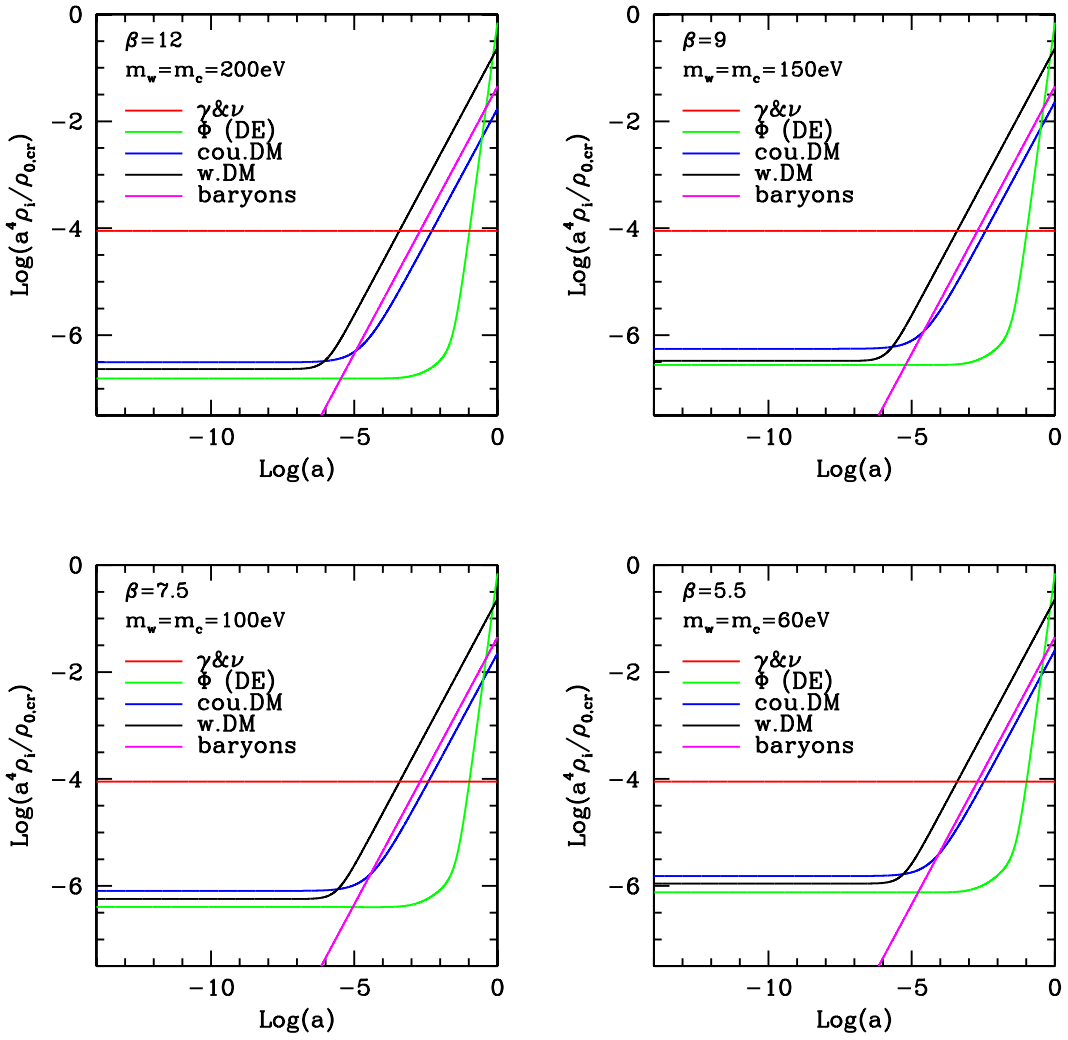


Figure 4: Density evolution of all components in some SCDEW models. Model parameters are shown in the boxes.

4. Linear fluctuation evolution

Fluctuation evolution in SCDEW models was first discussed in [7]. Further points were then outlined in [9], where models were modified to allow N–body simulations [10]. This was done by requiring DM–Φ interactions to rapidly vanish at a suitable redshift $z < 10^4$. Here, rather than suggesting such *ad–hoc* prescription, we show that β is rapidly cut off to quite low values, when the coupled DM field acquires a Higgs' mass. This is one of the main points of this work.

Initial conditions outside the horizon were treated by [7] and, in general, are to be quantitatively modified just for mass scales

$$M = \frac{4\pi}{3}\rho_m \left(\frac{2\pi}{k}\right)^3 \tag{4.1}$$

(ρ_m : sum of material component densities at $z = 0$) close to today's horizon. In a

synchronous gauge, the cosmic metric reads

$$ds^2 = a^2(\tau)[d\tau^2 - (\delta_{ij} + h_{ij})dx_i dx_j)] \ , \tag{4.2}$$

τ being the conformal time, while gravity perturbation is described by the 3–tensor h_{ij}, whose trace is h. The system of differential equations is also to be modified to take into account variable β's and the linear code already used by [7] and [9] was then modified accordingly. Let us remind that DE field fluctuations need also to be considered.

Let then

$$\phi = \Phi + \frac{b}{m_p}\varphi \ , \tag{4.3}$$

be the sum of the background field Φ considered in the previous Section and a perturbation described by φ. At the first perturbative order, the latter ϕ component fulfills an equation containing the term $a^2V''(\Phi)\varphi$, i.e. including the second derivative (in respect to Φ) of the self–interaction potential.

This is a critical point we wish to recall, for we prefer to refer to the $w(a)$ behavior and, therefore, as in [7], we replace

$$2V'' = \frac{A}{1+A}\left\{\frac{\dot{a}}{a}\frac{\epsilon}{1+A}\left[\epsilon_6\frac{\dot{a}}{a^3} + 2C\frac{\rho_c}{\dot{\Phi}}\right] + \left[\frac{\dot{a}}{a^3}\frac{\ddot{\Phi}}{\dot{\Phi}} + \frac{d}{d\tau}\left(\frac{\dot{a}}{a^3}\right)\right]\epsilon_6 + 2C\frac{\dot{\rho}_c}{\dot{\Phi}}\right\} \tag{4.4}$$

with A and ϵ defined as in eq. (2.9). Here $\epsilon_6 = \epsilon - 6$, while ρ_c is the coupled DM density.

Here again the background field Φ appears just through its derivatives. The φ and δ_c equations are also to be added the terms arising from the dependence of β (now β_{eff}) on Φ (eq. 2.25) and the public algorithm CMBFAST [20] is modified accordingly. For this work we used the version including tensor perturbations.

4.1 CMB

By using modified CMBFAST we obtain CMB spectra arising from scalar and tensor perturbations and compare them with LCDM. As it is known, this model parameters are fitted, first of all, to CMB data. All through this paper we kept the values of the basic parameters Ω_b, Ω_Φ, h, n_s, σ_8, etc., to the same values used for LCDM which, in turn, were the best fit values obtained in the Planck experiment [21]. In upper frame of Figure 5 we show the basic TT, TE, EE spectra; in the bottom frame, the tensor spectra are also shown. This kind of plots are insufficient to exhibit the tiny differences between SCDEW and LCDM.

In Figure 6 we then show the relative differences between TT spectra, keeping $m_w = 100\,\mathrm{eV}$, but considering different couplings. Differences are stronger for lower coupling, reaching $\sim 2\,\%$ for $\beta = 7$ and $\sim 4.5\,\%$ for $\beta = 4$ (not shown). Of course, this does not mean that low–coupling SCDEW cosmologies do not fit CMB data. Rather, direct tests of model outputs vs available data should be performed. We however expect some minor variation of the best fit cosmological parameter values, namely of the overall fluctuation normalization, well within 2–σ's, and no significant variation of the best fit likelihood.

A possible explanation of the "better performance" of large coupling is the smaller amount of coupled DM in fluctuations passing through the Last Scattering Band.

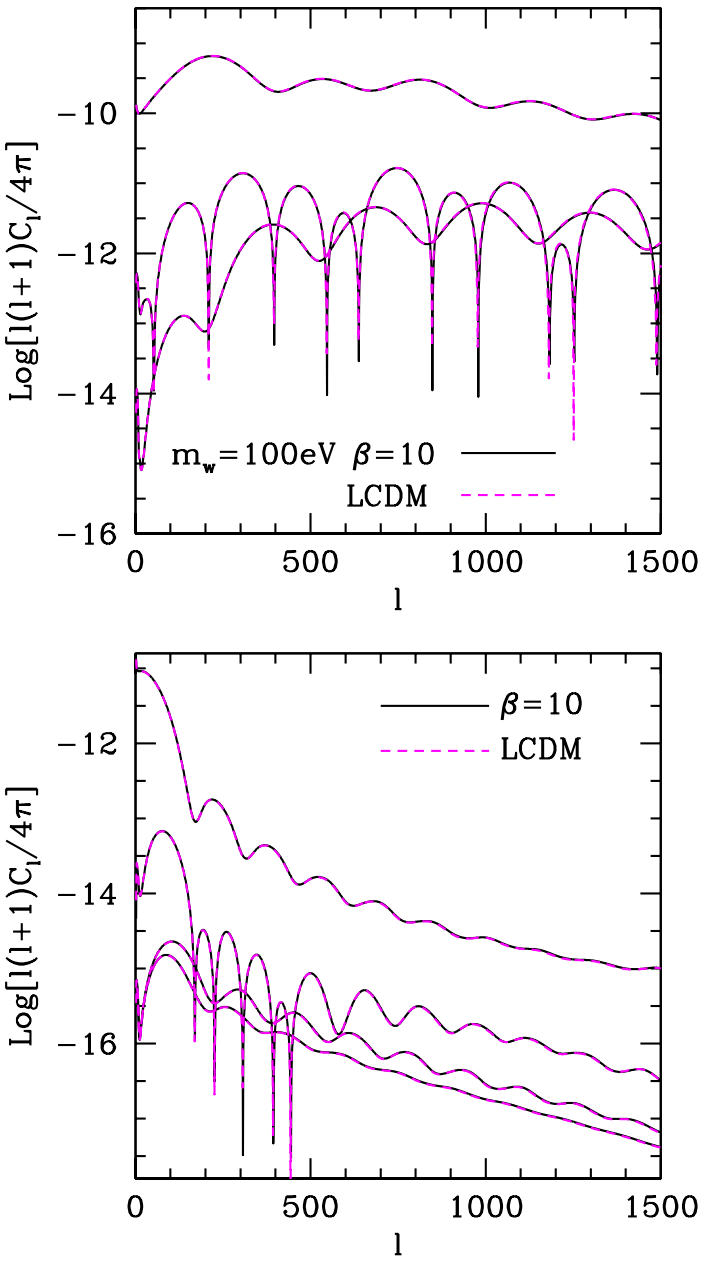


Figure 5: CMB spectra compared; LCDM vs. SCDEW with $m_{w,c} = 100$ eV and $\beta = 10$. Minimal differencies (see next plot) are essentially independent from $m_{w,c}$, and decreasing when greater β values are taken.

4.2 Linear spectra

Let us then tentatively compare SCDEW and LCDM fluctuation spectra at $z = 0$. We shall take into account also data from the 2dF redshift survey and Lyman–α analysis [22, 23], so to compare SCDEW–LCDM discrepancies with observational trends and errors. Seeking the best fit values of the SCDEW parameters (e.g., $m_{w,c}$ and β) by using available datasets,

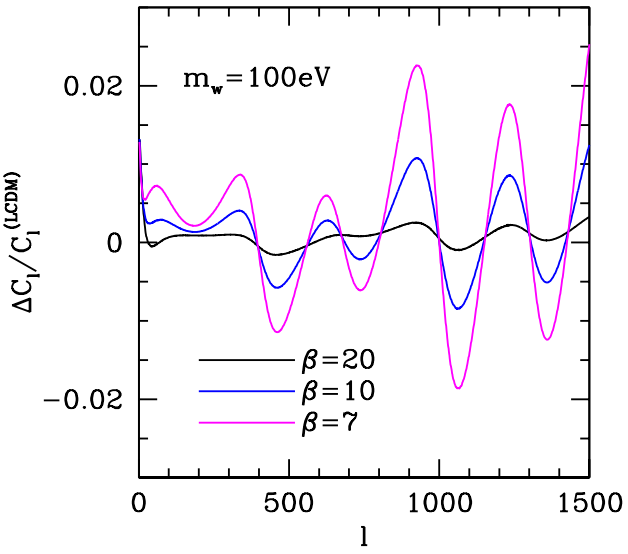


Figure 6: Fractional discrepancies between TT spectra for SCDEW and LCDM.

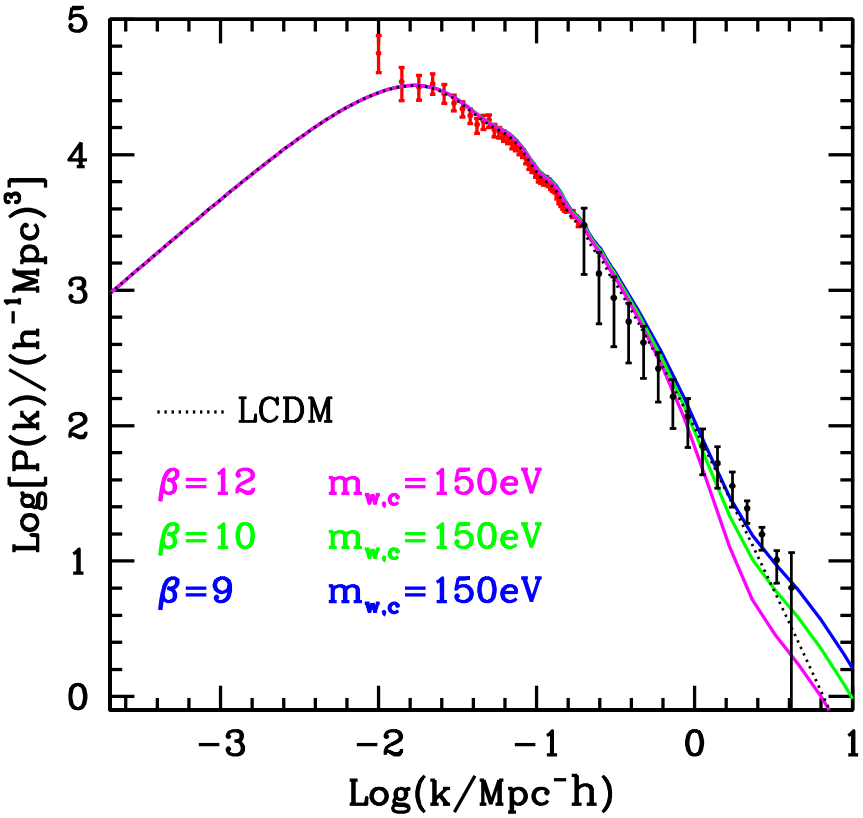


Figure 7: SCDEW and LCDM spectra vs. 2dF (in red) and Lyman–α (in black) data.

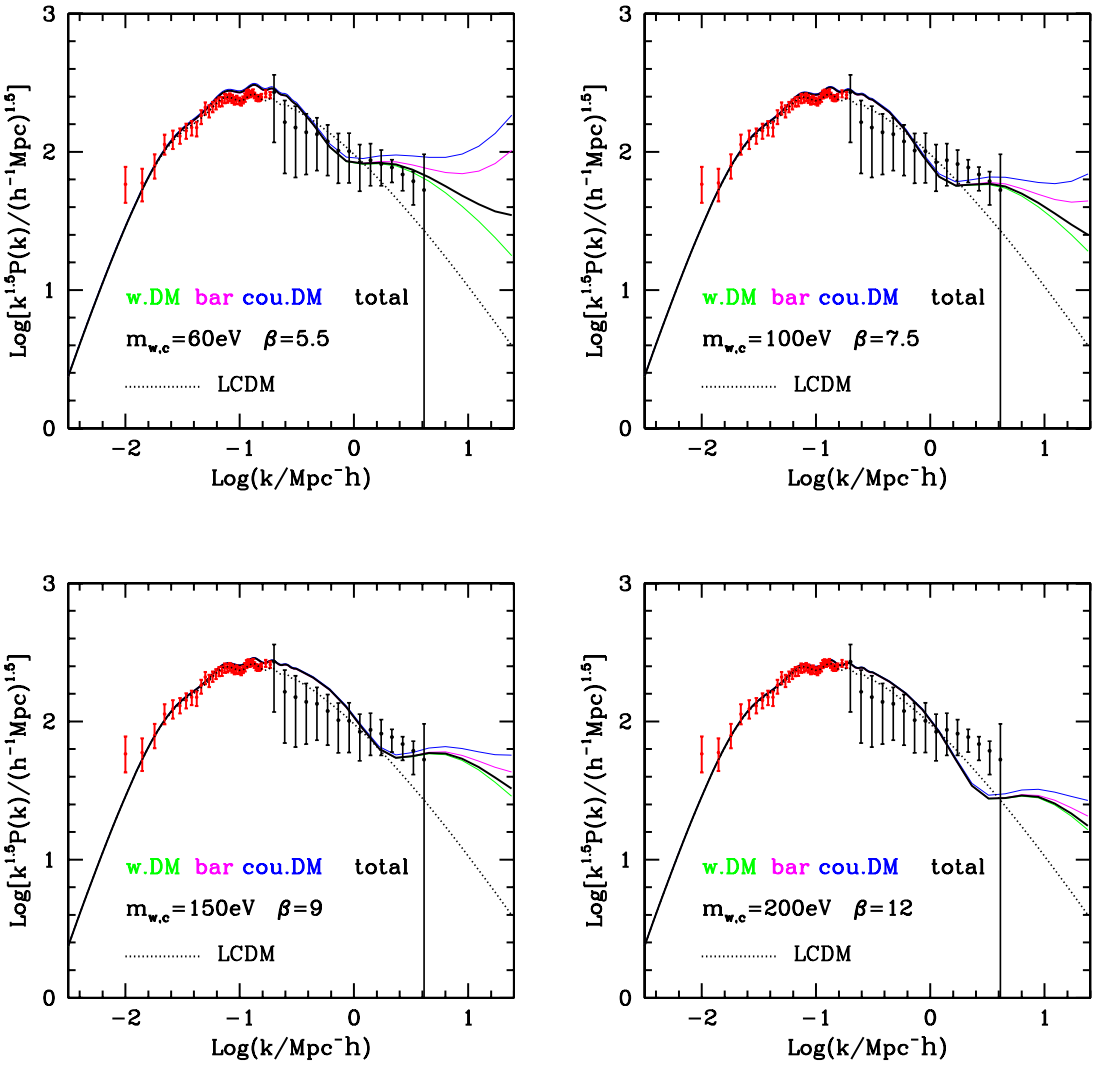


Figure 8: SCDEW and LCDM spectra vs. 2dF (in red) and Lyman–α (in black) data. Spectra are obtained from linear programs up to fairly large k values.

is out of our scopes in this analysis. Let us also outline that the physical mechanisms yielding SCDEW spectral shapes are discussed in the next Subsection.

In Figure 7 we then show the spectra for three SCDEW models and LCDM vs. data. The aim of this Figure is to illustrate how models depend on the value of the β parameter. Henceforth we keep $m_{w,c} \equiv 150\,\mathrm{eV}$ while the couplings $\beta = 9,\ 10,\ 12$ are considered. At large scale ($k <\sim 0.05\,h\,\mathrm{Mpc}^{-1}$) SCDEW–LCDM discrepancies are small and data are similarly fit by LCDM and SCDEW. For greater k values, however in the region where Lyman–α data are available, the fit appears better for smaller β's. At still greater k values, SCDEW spectra tend to exceed LCDM and to do more so for smaller β values.

The excess power for $\beta \sim 9$ concern scales which, in the present epoch, have reached the non–linear regime. Accordingly, it could indicate an early formations of galaxies, groups

and small clusters. Let us however outline that the fit of $z = 0$ spectra with Lyman–α data, concerning large–z systems, is slightly biased by the use of fluctuation evolution in a LCDM cosmology.

Further comparisons are provided in Figure 8, by plotting $k^{3/2}P(k)$, instead of $P(k)$ for the same SCDEW cosmologies of Figure 4 (incidentally, a comparison between Figure 7 and 8 shows the extraordinary impact of the way how spectra are shown, in appreciating spectral distorsions).

The spectra shown, up to $m_{w,c} = 150\,\mathrm{eV}$, are quite close to LCDM and meet observational errorbars, at least, as well as it; but also the last model keeps inside 3 σ's, while we should also recall how Lyman–α data are extrapolated to $z = 0$.

These plots also allow us to appreciate that different components still exhibit different transfer functions at $z = 0$, although at large k values, an effect stronger for smaller couplings. Another point is that, in order that models approach data, masses and β must be simultanously increased. A greater mass value causes an earlier weekening of the Φ–ψ coupling, so that the final amplitude of coupled DM spectra is decreased.

It is however clear that the most significant discrepancies between SCDEW and LCDM shall mostly concern non–linear scales, so that discriminating between the two cosmologies requires a difficult interplay between spectral differences and baryon physics assumptions.

4.3 Linear and non–linear fluctuation evolution

In Figure 9 we show the evolution of fluctuations with comoving wavelengths $\lambda_0 = 8$ and $0.8\,h^{-1}\mathrm{Mpc}$ (approximately $k = 3.09$ and $30.9\,h\mathrm{Mpc}^{-1}$) for the above models with $m_{w,c} = 100$ and $200\,\mathrm{eV}$.

These plot show the basic mechanism allowing models with low mass WDM to yield structure down to quite small mass scales. This is due cDM fluctuations growth also during the so–called *stag–flation* epoch, when uncoupled DM fluctuations, even if made of fully non –relativistic materials, are stuck to their amplitude at the horizon entry.

This effect can be easily understood, at least in the non–relativistic regime. In fact, as outlined in [19], in such regime coupling is equivalent to an apparent increase of the effective gravitational constant, when forces acting between coupled DM particles are considered. In such interactions, the gravity constant G is to be replaced by

$$G^* = \gamma_{eff}\, G \quad \text{with} \quad \gamma_{eff} = 1 + 4\beta_{eff}^2/3\ . \tag{4.5}$$

Other gravitational forces, even involving coupled DM particles, are still ruled by the ordinary G. Furthermore, while the dynamical law $\mathbf{f} = \mathbf{p}'$ continues to hold (here *prime* indicates differentiation with respect to time t), the particle mass decrease in time yields

$$m\mathbf{v}' = \mathbf{f} + m\mathbf{v}\left|m'/m\right|\ , \tag{4.6}$$

so that, besides of gravitational forces, coupled DM particles receive an *extra push* due to the second term at the r.h.s., sometimes unappropriately called *friction* term.

Let us also outline that the G boosting factor $\gamma = 1 + 4\beta^2/3$ partially cancels the fact that coupled DM has a density parameter $\Omega_c \simeq 1/2\beta^2$, so that the factor

$$\gamma\Omega_c = 1/2\beta^2 + 2/3 \tag{4.7}$$

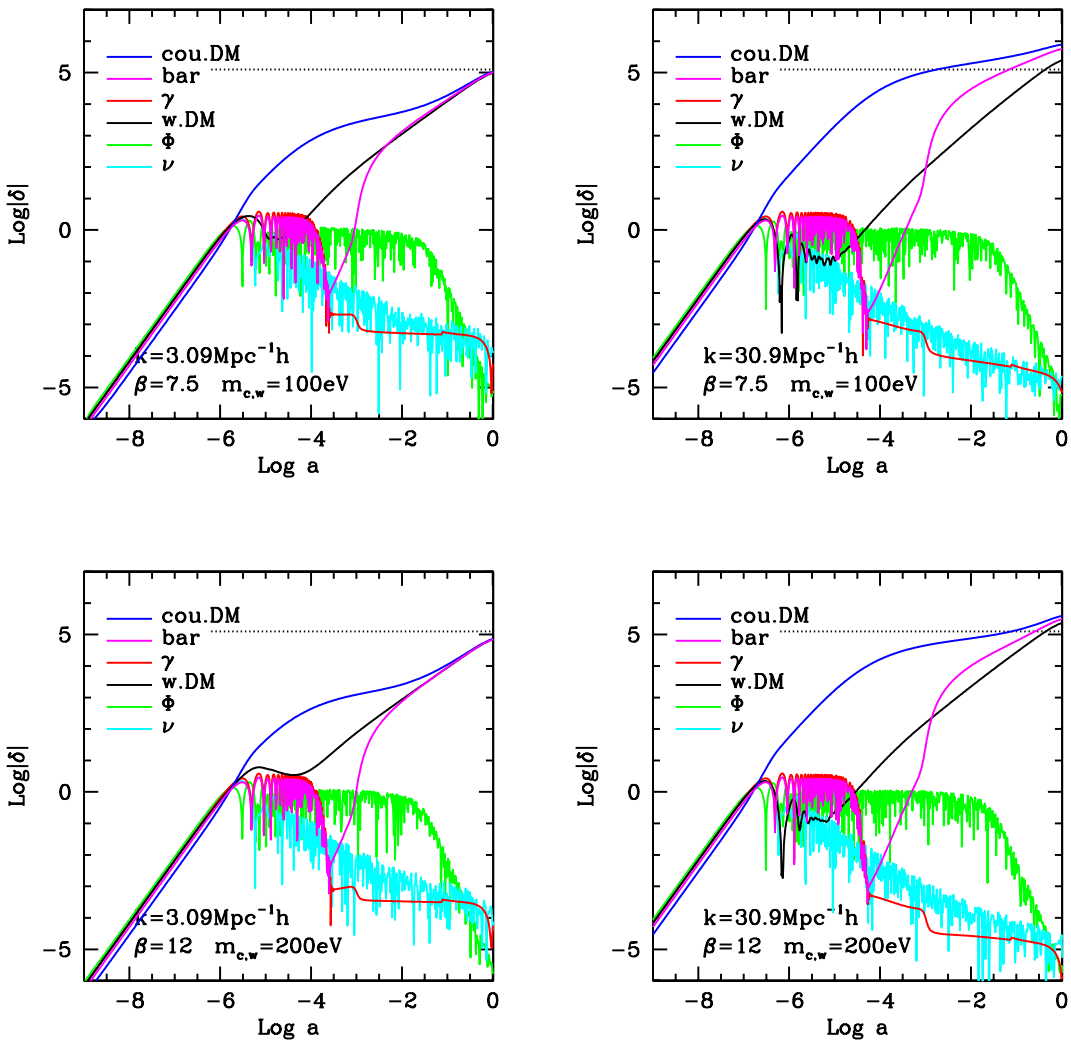


Figure 9: Linear evolution of fluctuations in SCDEW models. Magenta and green curves show γ and ν evolution, respectively. Matter components are colored as shown in the frames. Gravitational and Φ fields are omitted. The k scales considered are precisely 30.8935 and 3.08935 hMpc^{-1}, corresponding to 0.8 and 8 h^{-1}Mpc or to $\sim 1.79 \times 10^{11}$ and $1.79 \times 10^{14} h^{-2} M_\odot$, respectively.

multiplying $G = m_p^{-2}$, almost β–independent for large couplings, apparently indicates that cDM fluctuations evolve just as fluctuations with an amplitude reduced by a factor $\sim 2/3$, but concerning the whole critical density. But even the factor 2/3 is widely compensated by the *extra push*, so yielding the observed fast growth rate.

The dotted horizontal line, in Figures 9, shows where $\delta = 1$ if $\sigma_8 = 0.82$. This confirms that, at the scale of $8\,h^{-1}$Mpc, SCDEW models and LCDM are still fully compatible. Results are different at $0.8\,h^{-1}$Mpc. Here, in both models, coupled DM fluctuations attain non–linearity earlier than other non–relativistic components, while different components did not yet converge onto a single δ value, non–linearity is reached at different redshifts in the two models: in the case $\beta = 7.5$, infact, coupled CDM is already non–linear at $z \sim 1000$, for a scale of $\sim 10^{11} h^{-2} M_\odot$. On the contrary, in the model with $\beta = 12$, δ_c

attains non–linearity at $z \sim 100$.

This has an evident impact on the techniques used to analyse non–linear evolution (e.g., N–body simulations) and is due to SCDEW models relying on cDM fluctuation persistence to revive warm–DM fluctuations –at $z < z_{der} \sim 6 \times 10^5 (m_w/100\,\mathrm{eV})^{4/3} (\Omega_w h^2)^{-1/3}$– and baryon fluctuations, when they decoupled from γ's. This is the key effect, overcoming the former erasing of fluctuations in such components because of free streaming and sonic wave damping, respectively. However, if cDM fluctuations enter non–linearity too early, there is a numerical problem to evaluate fluctuation evolution and, possibly, a physical problem.

Clearly, cDM non–linearities depend on the mass scale. Over very large mass scales, average fluctuations have not yet entered non–linearity even today. A safe boundary is $\simeq 2 \times 10^{14} h^{-2} M_\odot$, as shown by the plots in the first column in Figure 9. At any smaller mass scales the redshift where cDM attains non linearity depends on model parameters, being smaller for greater $\tilde{\mu}$. When this occurs, linear predictions on all components are unsafe, although it should be reminded that $\delta_c > 1$ does not mean that the overall fluctuation $\delta > 1$. Furthermore, as shown in the second associated paper, the top density contrast of the coupled component could be just $\mathcal{O}(20)$, so hardly causing, by itself, a $\delta > 1$.

It is however evident that, over scales $\lesssim 10^{10}$–$10^{11} h^{-2} M_\odot$, non–linear effects can occur earlier in SCDEW than in LCDM. As these scales are non–linear today, a greater spectral amplitude essentially means an earlier system formation. As a matter of fact, however, the rise of observable structures over such scales depends on the growth of baryonic fluctuations, whose dynamics is ruled by hydrodynamics and dissipative effects.

Such earlier non–linearity has also an impact on the formation of unconventional structures, e.g. large Black Holes; although one could suggest that these expected features meet recent findings at high–z [11, 24], predictions are hard to schematize and our only claim here is that these features cannot be considered as a model difficulty. This is however the most intricate scale range to treat and ends up around a mass scale $M_{min} \simeq 10$–$100\, h^{-2} M_\odot$, as we show below.

In the second related paper [8], we actually considered a spherical density enhancement entering the horizon so early to turn around and virialize before z_{der}. After determining the time needed to reach virialization, we discover a very peculiar feature: that virialized structures will eventually dissipate. The time elapsing from $\delta_c \sim 10^{-3}$ (redshift z_3) and virialization makes $z_3 \simeq 100 \times z_{vir}$. Moreover, for average size fluctuations, $z_3 \sim 0.1 \times z_{hor}$. Accordingly, while in LWDM models fluctuations are able to survive only if their size is reached by the horizon after z_{der}, the presence of coupled–DM in SCDEW models shifts the critical redshift from z_{der} to $\sim 10^4 z_{der}$, at least, so lowering by $\sim$ 12–14 orders of magnitude the mass scale of the minimal surviving WDM fluctuation.

At $z_{eq} \sim 2 \times 10^4$ (matter–radiation equality), the horizon mass is $\sim 10^{17} h^{-2} M_\odot$; then, at $z_{der} \sim 30$–$50\, z_{eq}$, the horizon mass has lowered to $\sim 10^{13} h^{-2} M_\odot$; a further jump along z by a factor 10^4, finally lowers M_{min} to $\sim 10\, h^{-2} M_\odot$. This semi–quantitative estimate however assumes an almost instant dissolution of fluctuations after virialization. If the time taken by such process is long, M_{min} could be even smaller. On the contrary, the time scales deduced through the study of spherical fluctuations, are just approximate. The above conservative estimate $M_{min} \simeq 10$–$100\, h^{-2} M_\odot$ is meant to cover us against any such

risk.

Altogether, while SCDEW models substantially overlap LCDM predictions over a wide range of scales, their comparison with LCDM becomes harder over scales $\lesssim 10^9$–$10^{10} h^{-2} M_\odot$. There is however a wide range of SCDEW models which can be expected to approach cosmological observables over the full range of scales. Discriminating between LCDM and these models requires further work involving non–linear baryon physics.

5. Discussion

In previous works, we considered Strongly Coupled DE models either with coupling persisting down to $z = 0$, or by introducing an *ad–hoc* fading of coupling at a fixed redshift. The latter option allowed us to perform N–body simulations without needing suitable modifications of standard programs. Here below, we shall provide some further comments to these simulation results.

In this work we however adopted a third option, already envisaged in the Appendix of [9], which appears simple and highly effective. Most of the detailed results of this paper cannot prescind from its use.

In order to understand its features, let us start from recalling that the distance between the Planck scale m_p and the Higgs scale m_H is a phenomenological fact lacking explanation. One of the elements in favor of Super–Symmetries, e.g., is that they allow to preserve such distance against radiative corrections; but the very distance is an *ad–hoc* prescription of the standard model. The masses acquired at the m_H scale are also spread over various orders of magnitude, ranging from heavy quark and intermediate boson masses, themselves $\mathcal{O}(m_H)$, down to the unknown neutrino masses $\ll 1\,\mathrm{eV}$. Attempts to go beyond the standard model for fundamental interactions are also motivated by the hope to get rid of such a mess of parameters.

Cosmology adds its own contribute to this anthology. In LCDM models, the exit from radiation dominated era is set by nonrelativistic particle densities; both baryonic and DM densities being set by the product of tuned particle masses and number densities. Therefore, assuming a twofold DM nature, at first sight, furtherly worsens an already intricated situation. In spite of that, in the literature, several authors did consider such option on purely phenomenological bases.

On the contrary, the world picture described by SCDEW models seems to ease the problem. Even letting apart the option of a common origin of coupled and uncoupled DM components, both of them require just similar number densities close to γ's or ν's. Once a single DM Higgs' mass $m_w = \mathcal{O}(100\,\mathrm{eV})$ is assumed for coupled and warm DM quanta, the total variable mass of the former particles reads

$$m_{eff} = \mu \exp[-(b/m_p)(\Phi - \Phi_p)] + m_w \tag{5.1}$$

while, more significantly, an exponential cut–off of the coupling constant follows. The point is that, once the coupled DM component acquires a Higgs' mass, also its coupling fades, according to the law:

$$C_{eff} = \frac{C}{1 + (\mu/m_w)\exp[C(\Phi - \Phi_p)]} \ . \tag{5.2}$$

Let us recall that the behavior of $\Phi - \Phi_p$ is fixed by dynamical equations, so that the choice of C and m_w also defines the residual today's (very weak) coupling.

Accordingly, the presence of coupling and a twofold DM component, in SCDEW, rather than complicating the cosmological scenario, already appears as a sort of rationalization. This, however, is not the only point in support of SCDEW cosmologies. The persistence of the DE field Φ with an energy density constantly $\mathcal{O}(10^{-2}\rho_{cr})$ through various redshift decades, suggests that it played a role at both ends of this stationarity era which, in SCDEW cosmologies, replaces the ordinary radiative era; henceforth, we can expect that such conformally invariant expansion is triggered by inflation end and reaches iself an end as a consequence of Higgs mass acquisitions. Meanwhile, the Φ increase is just logarithmic, so that its present value is $\mathcal{O}(60\,\Phi_p)$. Even more significantly, in the potential $V(\Phi)$, that we refrained from detailing (and is responsible for the transition of Φ from its early kinetic behavior to the contemporary potential behavior), there should appear suitable constants which also grew logarithmically, according to the renormalization group equations, from the inflationary to the present era. Accordingly, one could attempt to build specific models where the same potential $V(\Phi)$ exceeds the kinetic energy $\dot{\Phi}^2/2a^2$, when Φ is large enough, either during inflation or at the eve of the present epoch.

The attractor nature of the conformally invariant expansion was illustrated here by following the recovery of the tracking regime when the number of spin degrees of freedom of the primeval *thermal soup* drastically changes. The example taken was the transition of strongly interacting matter from the early quark–gluon plasma to a hadron gas. In this connection we also evaluated the expected relevance of some (mild) consequences on primeval BBN.

Among the points illustrated in this work, there are CMB spectra due to both scalar and tensor perturbations. Here we found just small discrepancies from LCDM, however greater for lower values of the coupling constant β (for some multipoles up to $\sim 2\,\%$ if $\beta \sim 7$ and $m_w = 100\,\mathrm{eV}$).

At variance from previous expectations, in this work we argue that the coupled DM component of very small scale fluctuations, entering the horizon early enough, undergo an authonomous evolution, ending up with their total dissipation. The whole process is intrinsically different from the well know *free–streaming* of relativistic particles from early inhomogeneities, as soon that their size is reached by the horizon scale. The process we envisage proceeds through two basic stages, described in more detail in a second associated paper: (i) The effective self–gravity of cDM, boosted by its very coupling, causes cDM fluctuation to grow, even when the other components form sonic waves or freely stream. Such growth reaches a non–linear regime, so yielding a density contrast between cDM fluctuations and average cDM density $\sim$ 25–26, at virialization. (ii) But cDM particle mass still decreases and virialized configurations are unstable: particle orbits necessarily widen, finally destroying the initial inhomogeneity.

This process can be interrupted only if other cosmic components are involved, before the dissolution is total. SCDEW models therefore predict a minimal mass scale, below which fluctuations should not survive the entry in the horizon. The scale below which fluctuations do not survive this process is much lower than the *free streaming* mass scale

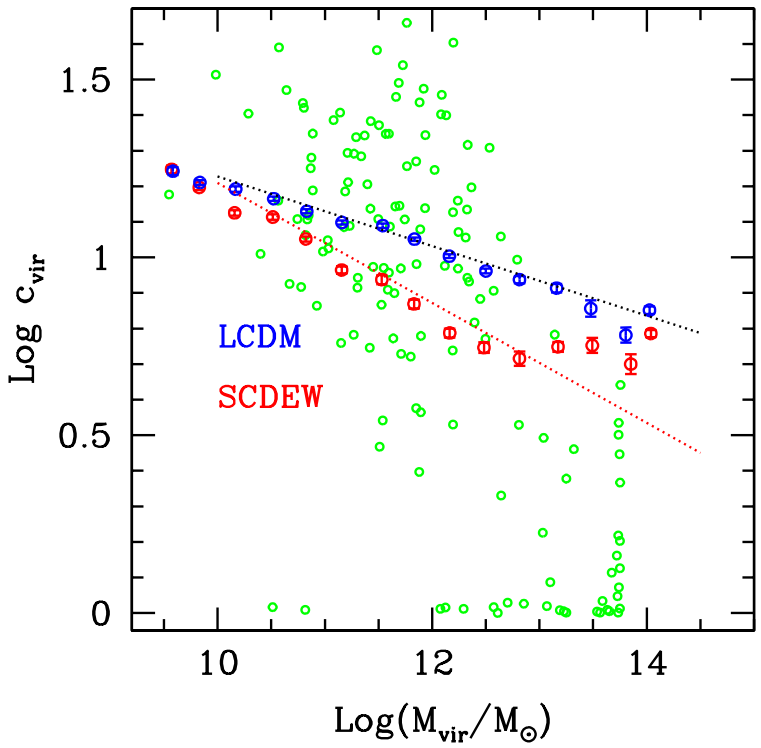


Figure 10: Halo concentrations predicted by SCDEW and LCDM N–body simulations vs. recent observational outputs, from the SPARC sample (courtesy of Katz et al. [25]). The large observational errors of data, provided in [25], are omitted. The visual impression that the LCDM fitting line is rather high and not sufficiently steep is confirmed by a more quantitative data analysis (see text).

for $\sim 100\,\mathrm{eV}$ particles in LWDM models, ranging around typical Pop III stellar mass scales.

This is why models involving such light particles can form adequate cosmic structures, as also shown by [10] through N–body simulations, performed for a model with $m_w = 90\,\mathrm{eV}$ and $\beta = 10$, assuming an *ad–hoc* complete coupling cut–off at $z \simeq 50$. As expected, DM being made of low mass particles significantly eases long standing problems. In particular: (i) simulated dwarf galaxy cores are much flatter than in LCDM; (ii) the number of MW–size galaxy satellites is reduced by a factor 0.3–0.5, fully adequate to fit their observed "scarsity"; (iii) the concentration distribution is also notably different. Here it may be worth peforming a comparison between the predicted concentration distribution, already shown by [10], and concentrations deduced by [25] from the SPARC dataset. This can be attempted on the basis of Figure 10 which seems to favor SCDEW, which provides a closer approximation to the rapid concentration decrease with mass.

In the Figure, observational point error bars, provided by [25], were omitted. The data spread, apparently much larger than simulations, could however be partially due to observational uncertainties. Virial mass values are derived from observational velocities, by assuming a NFW profile and a virial density contrast $\Delta_v = 98.7$, as in simulations. The

black and red dotted curves are fits of halo concentrations found in LCDM and SCDEW simulations, respectively. The former one meets all simulation points with an average quadratic deviation $\sim 10^{-2}$; the deviation for the latter one is ~ 4 times greater, essentially because of the 4 top mass points, which however include 75 over 4280 simulated halos (1.75 %). A requirement for a fair model is that the average quadratic deviations of observational points from simulation fitting lines, taken separately for points above and below the fits, are similar. Such ratio turns out to be 0.385 for LCDM and 1.000 for SCDEW; the latter value being even unexpectedly close to unity. This however confirms the visual impression that the LCDM fitting line is rather high and not sufficiently steep, in respect to data. From these computations, points with $\log c_{vir} < 0.01$ were omitted. We plan to perform a more detailed comparison in further work, also to test whether this kind of data provide any constraints on SCDEW model parameters.

We conclude that suitable SCDEW cosmologies, overlapping LCDM predictions for scales $\gtrsim 10^{12} h^{-2} M_{\odot}$ can be expected to be quite close to them down to galactic scales. They therefore provide an excellent fit of CMB and fluctuation spectral data. The point being that the new parameters of SCDEW can be suitably used to improve data fitting. At still smaller scales we can however outline a parameter independent SCDEW prediction, that small galaxies form earlier in SCDEW than in LCDM cosmologies, and that there ought to be a primeval spectrum low–scale cutoff around the mass scale of Pop III stars.

Acknowledgements: Thanks are due to Harley Katz and collaborators for providing us the concentration data files. Andrea Macciò is to be thanked for useful discussions, namely on this very point. We also acknowledge Sergio Monai's help in the graphic treatment of some datasets.

References

[1] see, e.g., L. Amendola, 1999, PRD 60, 043501; T. Chiba, 1999, PRD 60, 083508; N. Bartolo & M. Pietroni, 2000, PRD 61, 023518; F. Perrotta, C. Bagigalupi & S. Matarrese, PRD 61, 023607; G. Esposito & D. Polarski, 2001, PRD 63, 063504; S.M. Carrol, A.. DeFelice, V. Duvvuri, D.A. Easson, M. Trodden & M.S. Turner, 2006, JCAP 0608, 005; L. Amendola, R. Gannouji, D. Polarski & S. Tsujikawa, 2007, PRD 75, 083504; W. Hu & I. Sawicki, 2007, PRD 76, 064004; A. Starobinsky, JEPT Lett 86, 157; S.A. Appleby & R.A. Battye, 2007, Ph.Lett B 654, 7; V. Miranda, S.E. Joras, I. Waga & M. Quartin, 2009, PR Lett. 102, 2211; see also: L. Amendola & S. Tsujikawa, 2010, Dark Energy, Cambridge University Press.

[2] see, e.g.: L.Randall & R. Sundrum, 1999, Ph.R.Lett. 83, 3370 & 4690; P. Binetruy, C. Defayet & Langlois, 2000, Nuc.Ph.B 565, 269; P. Binetruy, C. Defayet, U. Ellwanger & Langlois, 2000, PHys.Lett B 477, 285; G.R. Dvali, G. Gabadadze & M. Porrati, 2000, Phys.Lett. B 485, 208; C. Deffayet, G.R. Dvaali & G. Gabadadze, 2002, PRD 65, 044023; see also: C. Rovelli, Quantum Gravity, 2004, Cambridge University Press

[3] see, e.g., Ellis J., S. Kalara, K.A. Olive & C. Wetterich, 1989, Ph.L.B 228, 264; Ratra B. & Peebles P.J.E., 1988, PRD 37, 3406; Wetterich C., 1995, A&A **301**, 321; L. Amendola, 2010, Dark Energy, Cambridge University Press.

[4] Amendola L., 1999, Ph.Rev. D **60**, 043501; Amendola L., 2000, Ph.Rev. D**62**, 043511; Amendola L., Tocchini-Valentini D., 2002 Phys.Rev. D66, 043528;

[5] A.V. Macció, C. Quercellini, R. Mainini, L. Amendola & S.A. Bonometto, 2004, arXiv:astro-ph/0309671 & PRD69, 123516; see also: M. Baldi, V. Pettorino, G. Robbers & V. Springel, 2010, MNRAS 403, 1684B

[6] Silvio A. Bonometto, Giandomenico Sassi, Giuseppe La Vacca, 2012, arXiv:1206.2281 & JCAP 08, 015

[7] Silvio A. Bonometto, Roberto Mainini, 2014, arXiv:1311.6374 & JCAP 03, 38

[8] Silvio A. Bonometto, Roberto Mainini, 2017, arXiv...., *Growth and dissolution of spherical density enhancements in SCDEW cosmologies*

[9] Silvio A. Bonometto, Roberto Mainini, Andrea V. Macció, 2015, arXiv:1503.07875 & MNRAS 453, 1002

[10] Andrea V. Macció, Roberto Mainini, Camilla Penzo, Silvio A. Bonometto, 2015, arXiv:1503.07867 & MNRAS 453, 1371

[11] See, e.g., Pallottini A., Ferrara A., Gallerani S., Salvadori S., DOdorico V., 2014, MNRAS 440, 2498; Pallottini A., et al., 2015, MNRAS 453, 2465; Sobral D., et al., 2015, ApJ 808, 139.

[12] See, e.g., Xia J.Q., 2013, JCAP 11, 22

[13] S. Das, P.S. Corasaniti & J. Khouri, 2006, PRD 73, 083509

[14] see, e.g., P. Petreszky, 2013, Proceedings of the X conference on Quark Confinement and Hadron Spectrum, October 2012, arXiv:1301.6188v1

[15] Silvio A. Bonometto & Roberto Mainini, 2016, arXiv:1610.05519 & Universe 4, 32

[16] see, e.g., J.P. Bernstein, R. Kessler, S. Kuhlmann, et al., 2012, ApJ 753, 152

[17] M. Demianski, E. Piedipalumbo, D. Sawant & L. Amati, 2016, arXiv:1609.09631 and A&A in press, see also: arXiv:1610.00854

[18] R. Laureijs, 2011, arXiv:1110.3193 *Euclid Definition Study Report.*

[19] A.V. Macció, C. Quercellini, R. Mainini, L. Amendola, S.A. Bonometto, 2004, Phys.R. D69, 123516, and arXiv:astro–ph/0309671

[20] U. Seljak & M. Zaldarriaga, 1996, ApJ 469, 437; M. Zaldarriaga, U. Seljak & E. Bertschinger, 1998, ApJ 494, 491; M. Zaldarriaga & U. Seljak, 2000, ApJ Supp. 129, 431.

[21] Planck collaboration, 2015, arXiv:1502.01589v3.

[22] S. Cole et al., 2005, arXiv:astro–ph/0501174 & MNRAS 362, 505

[23] S. Zaroubi, M. Viel, A. Nusser, M. Haehnelt & T.-S Kim, 2006, arXiv:astro–ph/0509563v3 & MNRAS 369, 734

[24] See, e.g., Pacucci F., Pallottini A., Ferrara A. & Gallerani S., 2017, arXiv:1702.04351, MNRAS Lett. (in press) and references therein.

[25] Katz H., Lelli F., McGauch S.S., Di Cintio A., Brook C.B. Schombert J.M., 2016, arXiv:1605.05971, *Testing Feedback–Modified Dark Matter Haloes with Galaxy Rotation Curves: Estimation of Halo Parameters and Consistency with LCDM*